



Analytical Solution for Wave Propagation in Stratified Acoustic/Porous Media. Part I: the 2D Case

Julien Diaz, Abdelaâziz Ezziani

► To cite this version:

Julien Diaz, Abdelaâziz Ezziani. Analytical Solution for Wave Propagation in Stratified Acoustic/Porous Media. Part I: the 2D Case. [Research Report] RR-6509, 2008, pp.28. inria-00274136v2

HAL Id: inria-00274136

<https://inria.hal.science/inria-00274136v2>

Submitted on 21 Apr 2008 (v2), last revised 28 Jul 2008 (v3)

HAL is a multi-disciplinary open access archive for the deposit and dissemination of scientific research documents, whether they are published or not. The documents may come from teaching and research institutions in France or abroad, or from public or private research centers.

L'archive ouverte pluridisciplinaire **HAL**, est destinée au dépôt et à la diffusion de documents scientifiques de niveau recherche, publiés ou non, émanant des établissements d'enseignement et de recherche français ou étrangers, des laboratoires publics ou privés.

INSTITUT NATIONAL DE RECHERCHE EN INFORMATIQUE ET EN AUTOMATIQUE

*Analytical Solution for Wave Propagation in
Heterogeneous Acoustic/Porous Media. Part I: the
2D Case*

Julien Diaz — Abdelaâziz Ezziani

N° 6509

Avril 2008

Thème NUM



Analytical Solution for Wave Propagation in Heterogeneous Acoustic/Porous Media. Part I: the 2D Case

Julien Diaz^{*} †, Abdelaâziz Ezziani^{† *}

Thème NUM — Systèmes numériques
Équipe-Projet Magique-3D

Rapport de recherche n° 6509 — Avril 2008 — 25 pages

Abstract: We are interested in the modeling of wave propagation in an infinite bilayered acoustic/poroelastic media. We consider the biphasic Biot's model in the poroelastic layer. This first part is devoted to the calculation of analytical solution in two dimensions, thanks to Cagniard de Hoop method. The solution is validated through comparison with solutions obtained by a numerical code. In the second part we'll consider the 3D case.

Key-words: Biot's model, poroelastic waves, acoustic waves, acoustic/poroelastic coupling, analytical solution, Cagniard-De Hoop's technique.

* EPI Magique-3D, Centre de Recherche Inria Bordeaux Sud-Ouest

† Laboratoire de Mathématiques et de leurs Applications, CNRS UMR-5142, Université de Pau et des Pays de l'Adour – Bâtiment IPRA, avenue de l'Université – BP 1155-64013 PAU CEDEX

Solution analytique pour la propagation d'ondes en milieu hétérogène acoustique/poroélastique. Partie I : en dimension 2

Résumé : Nous nous intéressons à la modélisation de la propagation d'ondes dans les milieux infinis bicouche acoustique/poroélastique. Nous considérons le modèle bi-phasique de Biot dans la couche poroélastique. Cette première partie est consacrée au calcul de la solution analytique en dimension deux à l'aide de la technique de Cagniard-De Hoop. Cette solution a été validée à l'aide de comparaisons avec des solutions obtenues par un code numérique. Dans la seconde partie de ce rapport nous traiterons le cas de la dimension trois.

Mots-clés : Modèle de Biot, ondes poroélastiques, ondes acoustiques, couplage acoustique/poroélastique, solution analytique, technique de Cagniard de Hoop.

Introduction

The computation of analytical solution for wave propagation problems is of high importance for the validation of numerical computational codes or for a better understanding of the reflexion/transmission properties of the media. Cagniard-de Hoop method [4, 6] is a useful tool to obtain such solutions and permits the independent computation of each type of waves (P wave, S wave, head wave...), moreover it makes a link between transient and plane wave. Although it was originally dedicated to the solution of elastodynamic wave propagation, it can be applied to any transient wave propagation problem in stratified medium. However, as far as we know, there are very few works dedicated to the application of this method to poroelastic medium. In [9] the analytical solution of poroelastic wave propagation in an homogeneous 2D medium is provided and in [10] the authors compute the analytical solution of the reflected wave at the interface between an acoustic and a poroelastic layer in two dimension but they do not explicit the solution of the transmitted waves.

In order to validate computational codes of wave propagation in poroelastic media, we have implemented the codes Gar6more 2D [8] and Gar6more 3D which provide the complete solution (reflected and transmitted waves) of the propagation of wave in stratified 2D or 3D media composed of acoustic/acoustic, acoustic/elastic, acoustic/poroelastic or poroelastic/poroelastic layers. The 2D code is freely downloadable at

<http://www.spice-rtn.org/library/software/Garcimore2D>.

We will focus here on the 2D acoustic/poroelastic case, the three dimensional and the poroelastic case will be the object of forthcoming papers. The outline of the paper is as follows: we first present the model problem we want to solve and derive the Green problem from it (section 1). Then we present the analytical solution of wave propagation in a stratified 2D medium composed of an acoustic and a poroelastic layer (section 2). Finally we validate our results through comparison with a numerical solution(section 3).

1 The model problem

We consider an infinite two dimensional medium ($\Omega = \mathbf{R}^2$) composed of an acoustic layer $\Omega^+ = \mathbf{R} \times]-\infty, 0]$ and a poroelastic layer $\Omega^- = \mathbf{R} \times [0, +\infty[$ separated by an horizontal interface Γ (see Fig. 1). We first describe the equations in the two layers (§1.1 and §1.2) and the transmission conditions on the interface Γ (§1.3), then we will present the Green problem from which we will compute the analytical solution (§1.4).

1.1 The equation of acoustics

In the acoustic layer we consider the second order formulation of the wave equation with a point source and zero initial conditions:

$$\ddot{P}^+ - V^{+2} \Delta P^+ = \delta_x \delta_{y-h} f(t), \quad \text{in } \Omega^+ \times]0, T], \quad (1a)$$

$$\ddot{\mathbf{U}}^+ = -\frac{1}{\rho^+} \nabla P^+, \quad \text{in } \Omega^+ \times]0, T], \quad (1b)$$

$$P^+(x, y, 0) = 0, \dot{P}^+(x, y, 0) = 0, \quad \text{in } \Omega^+ \quad (1c)$$

$$\mathbf{U}^+(x, y, 0) = 0, \dot{\mathbf{U}}^+(x, y, 0) = 0, \quad \text{in } \Omega^+ \quad (1d)$$

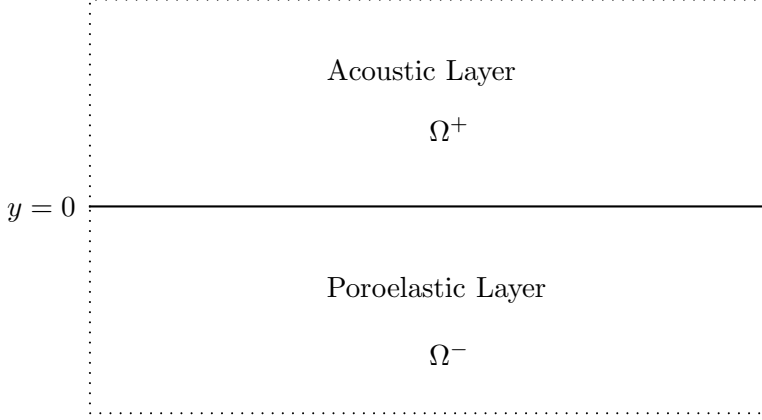


Figure 1: Configuration of the study

where

- P^+ is the pressure;
- \mathbf{U}^+ is the displacement field;
- V^+ is the celerity of the wave;
- ρ^+ is the density of the fluid.

1.2 Biot's Model

In the second layer we consider the second order formulation of the poroelastic equations [1, 2, 3]

$$\rho^- \ddot{\mathbf{U}}_s^- + \rho_f^- \ddot{\mathbf{W}}^- - \nabla \cdot \Sigma^- = 0, \quad \text{in } \Omega^- \times]0, T], \quad (2a)$$

$$\rho_f^- \ddot{\mathbf{U}}_s^- + \rho_w^- \ddot{\mathbf{W}}^- + \frac{1}{\mathcal{K}^-} \dot{\mathbf{W}}^- + \nabla P^- = 0, \quad \text{in } \Omega^- \times]0, T], \quad (2b)$$

$$\Sigma^- = \lambda^- \nabla \cdot \mathbf{U}_s^- \mathbf{I}_2 + 2\mu^- \varepsilon(\mathbf{U}_s^-) - \beta^- P^- \mathbf{I}_2, \quad \text{in } \Omega^- \times]0, T], \quad (2c)$$

$$\frac{1}{m^-} P^- + \beta^- \nabla \cdot \mathbf{U}_s^- + \nabla \cdot \mathbf{W}^- = 0, \quad \text{in } \Omega^- \times]0, T], \quad (2d)$$

$$\mathbf{U}_s^-(x, 0) = 0, \quad \mathbf{W}^-(x, 0) = 0, \quad \text{in } \Omega^-, \quad (2e)$$

$$\dot{\mathbf{U}}_s^-(x, 0) = 0, \quad \dot{\mathbf{W}}^-(x, 0) = 0, \quad \text{in } \Omega^-, \quad (2f)$$

with

$$(\nabla \cdot \Sigma^-)_i = \sum_{j=1}^2 \frac{\partial \Sigma_{ij}^-}{\partial x_j} \quad \forall i = 1, 2, \quad \mathbf{I}_2 \text{ is the identity matrix of } \mathcal{M}_2(\mathbb{R}),$$

and $\varepsilon(\mathbf{U}_s^-)$ is the solid strain tensor defined by:

$$\varepsilon_{ij}(\mathbf{U}) = \frac{1}{2} \left(\frac{\partial U_i}{\partial x_j} + \frac{\partial U_j}{\partial x_i} \right).$$

In (2), the unknowns are:

- \mathbf{U}_s^- the displacement field of solid particle;
- $\mathbf{W}^- = \phi^-(\mathbf{U}_f^- - \mathbf{U}_s^-)$, the relative displacement, \mathbf{W}_f^- being the displacement field of fluid particle and ϕ^- the porosity;
- P^- , the fluid pressure;
- Σ^- , the solid stress tensor.

The parameters describing the physical properties of the medium are as follows:

- $\rho^- = \phi^- \rho_f^- + (1 - \phi^-) \rho_s^-$ is the overall density of the saturated medium, with ρ_s^- the density of the solid and ρ_f^- the density of the fluid;
- $\rho_w^- = a^- \rho_f^- / \phi^-$, a^- the porosity of the solid matrix;
- $\mathcal{K}^- = \kappa^- / \eta^-$, κ^- is the permeability of the solid matrix and η is the viscosity of the fluid;
- m^- and β^- are positive physical coefficients: $\beta^- = 1 - K_b^- / K_s^-$
and $m^- = [\phi^- / K_f^- + (\beta^- - \phi^-) / K_s^-]^{-1}$, where K_s^- is the bulk modulus of the solid,
 K_f^- is the bulk modulus of the fluid and K_b^- is the frame bulk modulus;
- μ^- is the frame shear modulus, and $\lambda^- = K_b^- - 2\mu^- / 3$ is the Lame constant.

1.3 Transmission conditions

Let \mathbf{n} be the normal of Γ exterior of Ω^- . The transmission conditions on the interface between the acoustic and porous medium are [5] :

$$\begin{cases} \mathbf{W}^- \cdot \mathbf{n} = (\mathbf{U}^+ - \mathbf{U}_s^-) \cdot \mathbf{n}, \\ P^- = P^+, \\ \Sigma^- \mathbf{n} = -P^+ \mathbf{n}. \end{cases} \quad (3)$$

1.4 The Green problem

We won't compute directly the solution of (1-2-3) but the solution of the Green problem:

$$\ddot{p}^+ - V^{+2} \Delta p^+ = \delta_x \delta_{y-h} \delta_t, \quad \text{in } \Omega^+ \times]0, T], \quad (4a)$$

$$\ddot{\mathbf{u}}^+ = -\frac{1}{\rho^+} \nabla p^+, \quad \text{in } \Omega^+ \times]0, T], \quad (4b)$$

$$\rho^- \ddot{\mathbf{u}}_s^- + \rho_f^- \ddot{\mathbf{w}}^- - \nabla \cdot \sigma^- = 0, \quad \text{in } \Omega^- \times]0, T], \quad (5a)$$

$$\rho_f^- \ddot{\mathbf{u}}_s^- + \rho_w^- \ddot{\mathbf{w}}^- + \frac{1}{\mathcal{K}^-} \dot{\mathbf{w}}^- + \nabla p^- = 0, \quad \text{in } \Omega^- \times]0, T], \quad (5b)$$

$$\sigma^- = \lambda^- \nabla \cdot \mathbf{u}_s^- \mathbf{I}_2 + 2\mu^- \varepsilon(\mathbf{u}_s^-) - \beta^- p^- \mathbf{I}_2, \quad \text{in } \Omega^- \times]0, T], \quad (5c)$$

$$\frac{1}{m^-} p^- + \beta^- \nabla \cdot \mathbf{u}_s^- + \nabla \cdot \mathbf{w}^- = 0, \quad \text{in } \Omega^- \times]0, T], \quad (5d)$$

$$\begin{cases} \mathbf{w}^- \cdot \mathbf{n} = (\mathbf{u}^+ - \mathbf{u}_s^-) \cdot \mathbf{n}, & \text{on } \Gamma \\ p^- = p^+, & \text{on } \Gamma \\ \sigma^- \mathbf{n} = -p^+ \mathbf{n}. & \text{on } \Gamma \end{cases} \quad (6)$$

The solution of (1-2-3) is then computed from the solution of the Green Problem thanks to a convolution by the source function. For instance we have :

$$P^+(x, y, t) = p^+(x, y, .) * f(.) = \int_0^t p^+(x, y, \tau) f(t - \tau) d\tau$$

We also suppose that the poroelastic medium is non dissipative, i.e the viscosity $\eta^- = 0$. Using the equations (5c,5d) we can eliminate σ^- and p^- in (5), we obtain the the equivalent system:

$$\begin{cases} \rho^- \ddot{\mathbf{u}}_s^- + \rho_f^- \ddot{\mathbf{w}}^- - \alpha^- \nabla(\nabla \cdot \mathbf{u}_s^-) + \mu^- \nabla \times (\nabla \times \mathbf{u}_s^-) - m^- \beta^- \nabla(\nabla \cdot \mathbf{w}^-) = 0, \\ \rho_f^- \ddot{\mathbf{u}}_s^- + \rho_w^- \ddot{\mathbf{w}}^- - m^- \beta^- \nabla(\nabla \cdot \mathbf{u}_s^-) - m^- \nabla(\nabla \cdot \mathbf{w}^-) = 0, \end{cases} \quad (7)$$

with $\alpha^- = \lambda^- + 2\mu^- + m^- \beta^{-2}$.

And using the equation (4b) the transmission conditions (6) are rewritten as:

$$\begin{cases} \ddot{u}_{sy}^- + \ddot{w}_y^- = -\frac{1}{\rho^+} \partial_y p^+, \\ -m^- \beta^- \nabla \cdot \mathbf{u}_s^- - m^- \nabla \cdot \mathbf{w}^- = p^+, \\ \partial_y u_{sx}^- + \partial_x u_{sy}^- = 0, \\ (\lambda^- + m^- \beta^-) \nabla \cdot \mathbf{u}_s^- + 2\mu^- \partial_y u_{sy}^- + m^- \nabla(\nabla \cdot \mathbf{w}) = -p^+. \end{cases} \quad (8)$$

We decompose the displacement fields \mathbf{u}_s^- et \mathbf{u}_f^- on irrotationnal and isovolumic fields (P-wave and S-wave):

$$\mathbf{u}_s^- = \nabla \Theta_u^- + \nabla \times \Psi_u^- ; \quad \mathbf{w}^- = \nabla \Theta_w^- + \nabla \times \Psi_w^-. \quad (9)$$

We can then rewrite the system (7) in the following form:

$$\begin{cases} A^- \ddot{\Theta}^- - B^- \Delta \Theta^- = 0, \\ \ddot{\Psi}_u^- - V_S^{-2} \Delta \Psi_u^- = 0, \\ \ddot{\Psi}_w^- = -\frac{\rho_f^-}{\rho_w^-} \ddot{\Psi}_u^-, \end{cases} \quad (10)$$

where Θ^- is a two vector: $\Theta = (\Theta_u^-, \Theta_w^-)^t$, A^- and B^- are two 2×2 symetric matrices:

$$A^- = \begin{pmatrix} \rho^- & \rho_f^- \\ \rho_f^- & \rho_w^- \end{pmatrix} ; \quad B^- = \begin{pmatrix} \lambda^- + 2\mu^- + m^- (\beta^-)^2 & m^- \beta^- \\ m^- \beta^- & m^- \end{pmatrix},$$

and

$$V_S^- = \sqrt{\frac{\mu \rho_w^-}{\rho^- \rho_w^- - \rho_f^-}}$$

is the S-wave velocity.

We multiply the first equation of the system (10) by the inverse of A . The matrix $A^{-1}B$ is diagonalisable: $A^{-1}B = \mathcal{P}D\mathcal{P}^{-1}$, where \mathcal{P} is the change-of-coordinate matrix, $D = \text{diag}(V_{Pf}^{-2}, V_{Ps}^{-2})$ is the diagonal matrix similar to $A^{-1}B$, V_{Pf}^- and V_{Ps}^- are respectively the fast P-wave velocity and the slow P-wave velocity ($V_{Ps}^- < V_{Pf}^-$).

Using the change of variables $\Phi = (\Phi_{Pf}, \Phi_{Ps})^t = \mathcal{P}^{-1}\Theta$, we obtain the decoupled system on fast P-wave, slow P-wave and S-wave:

$$\begin{cases} \ddot{\Phi} - D \Delta \Phi = 0, \\ \ddot{\Psi}_u^- - V_S^{-2} \Delta \Psi_u^- = 0, \\ \Psi_w^- = -\frac{\rho_f^-}{\rho_w^-} \Psi_u^-, \end{cases} \quad (11)$$

Finally, we obtain the Green problem equivalent to (4,5,6):

$$\begin{cases} \ddot{p}^+ - V^+{}^2 \Delta p^+ = \delta_x \delta_{y-h} \delta_t, & y > 0 \\ \ddot{\Phi}_i^- - V_i^-{}^2 \Delta \Phi_i^- = 0, \quad i \in \{PS, Pf, S\} & y < 0 \\ \mathcal{B}(p^+, \Phi_{Pf}^-, \Phi_{Ps}^-, \Phi_S^-) = 0, & y = 0 \end{cases} \quad (12)$$

where we have set $\Phi_S = \Psi_u$ in order to have similar notations for the Pf , Ps and S waves. The operator \mathcal{B} represents the transmission conditions on Γ :

$$\mathcal{B} \begin{pmatrix} p^+ \\ \Phi_{Pf}^- \\ \Phi_{Ps}^- \\ \Phi_S^- \end{pmatrix} = \begin{bmatrix} \frac{1}{\rho^+} \partial_y & (\mathcal{P}_{11} + \mathcal{P}_{21}) \partial_{ytt}^3 & (\mathcal{P}_{12} + \mathcal{P}_{22}) \partial_{ytt}^3 & \left(\frac{\rho_f^-}{\rho_w^-} - 1\right) \partial_{xtt}^3 \\ 1 & \frac{m^- (\beta^- \mathcal{P}_{11} + \mathcal{P}_{21})}{V_{Pf}^{-2}} \partial_{tt}^2 & \frac{m^- (\beta^- \mathcal{P}_{12} + \mathcal{P}_{22})}{V_{Ps}^{-2}} \partial_{tt}^2 & 0, \\ 0 & 2\mathcal{P}_{11} \partial_{xy}^2 & 2\mathcal{P}_{12} \partial_{xy}^2 & \partial_{yy}^2 - \partial_{xx}^2, \\ 1 & \mathcal{B}_{42} & \mathcal{B}_{43} & -2\mu^- \partial_{xy}^2 \end{bmatrix} \begin{pmatrix} p^+ \\ \Phi_{Pf}^- \\ \Phi_{Ps}^- \\ \Phi_S^- \end{pmatrix}$$

with

$$\mathcal{B}_{42} = \frac{(\lambda^- + m^- \beta^{-2}) \mathcal{P}_{11} + m^- \beta^- \mathcal{P}_{21}}{V_{Pf}^{-2}} \partial_{tt}^2 + 2\mu^- \mathcal{P}_{11} \partial_{yy}^2,$$

$$\mathcal{B}_{43} = \frac{(\lambda^- + m^- \beta^{-2}) \mathcal{P}_{12} + m^- \beta^- \mathcal{P}_{22}}{V_{Ps}^{-2}} \partial_{tt}^2 + 2\mu^- \mathcal{P}_{12} \partial_{yy}^2.$$

To obtain this operator we have used the transmisson conditions (8), the change of variables (9) and the decoupled system (11).

Moreover, we can determine the solid displacement \mathbf{u}_s^- by using the change of variables (9) and the fluid displacement \mathbf{u}^+ by using (4b).

2 Computation of the analytical solution

In this section we present the expression of the analytical solution of the Green problem (§2.2), the proof of the result is detailed at §2.3. To simplify the presentation of the theorem we have used some notations that we present at §2.1

2.1 Notations

To state our results, we need the following notation and definitions:

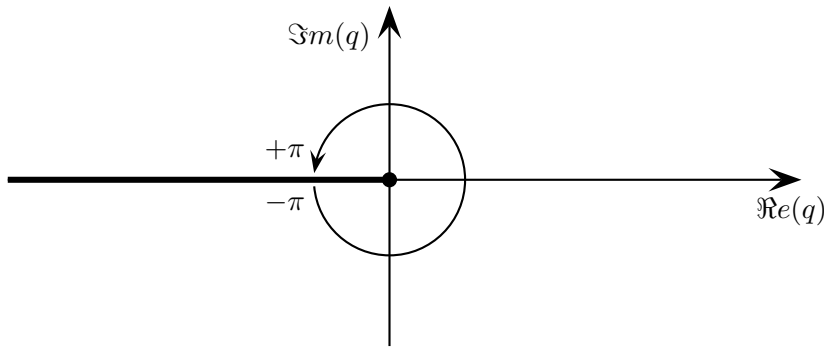
- 1. Definition of the complex square root.** For $q \in \mathbb{C} \setminus \mathbb{R}^-$, we use the following definition of the square root $g(q) = q^{\frac{1}{2}}$:

$$g(q)^2 = q \quad \text{and} \quad \Re e[g(q)] > 0.$$

The branch cut of $g(q)$ in the complex plane will thus be the half-line defined by $\{q \in \mathbb{R}^-\}$ (see Fig. 2). In the following, we'll use the notation abuse $g(q) = i\sqrt{q}$ for $q \in \mathbb{R}^-$.

- 2. Definition of the function κ^+ and κ_i^- .** For $i \in \{Pf, Ps, S\}$ and $q \in \mathbb{C}$, we define the functions

$$\kappa^+(q) = \left(\frac{1}{V^{+2}} + q^2 \right)^{\frac{1}{2}}.$$

Figure 2: Definition of the function $x \mapsto (x)^{\frac{1}{2}}$

and

$$\kappa_i^-(q) = \left(\frac{1}{V_i^{-2}} + q^2 \right)^{\frac{1}{2}}.$$

For a sake of simplicity, we'll omit sometimes the dependance in q and only write κ^+ and κ_i^- .

Remark 2.1. *The branch cuts of κ^+ are the two half lines*

$$\{q \in \mathbb{C} \mid \operatorname{Re}(q) = 0 \text{ and } |\operatorname{Im}(q)| \geq \frac{1}{V^+}\}$$

and the branch cuts of κ_i^- are the two half lines

$$\{q \in \mathbb{C} \mid \operatorname{Re}(q) = 0 \text{ and } |\operatorname{Im}(q)| \geq \frac{1}{V_i^-}\}$$

3. **Definition of the reflection and transmission coefficients.** For a given $q \in \mathbb{C}$, we denote by $\mathcal{R}(q)$, $\mathcal{T}_{Pf}(q)$, $\mathcal{T}_{Ps}(q)$ and $\mathcal{T}_S(q)$ the solution of the linear system

$$\mathcal{A}(q) \begin{bmatrix} \mathcal{R}(q) \\ \mathcal{T}_{Pf}(q) \\ \mathcal{T}_{Ps}(q) \\ \mathcal{T}_S(q) \end{bmatrix} = -\frac{1}{2\kappa^+ V^{+2}} \begin{bmatrix} \frac{\kappa^+}{\rho^+} \\ 1 \\ 0 \\ 1 \end{bmatrix}, \quad (13)$$

where the matrix $\mathcal{A}(q)$ is defined by:

$$\mathcal{A}(q) = \begin{bmatrix} -\frac{\kappa^+}{\rho^+} & \kappa_{Pf}^-(\mathcal{P}_{11} + \mathcal{P}_{21}) & \kappa_{Ps}^-(\mathcal{P}_{12} + \mathcal{P}_{22}) & i q \left(\frac{\rho_f^-}{\rho_w^-} - 1 \right) \\ 1 & \frac{m^-}{V_{Pf}^{-2}} (\beta^- \mathcal{P}_{11} + \mathcal{P}_{21}) & \frac{m^-}{V_{Ps}^{-2}} (\beta^- \mathcal{P}_{12} + \mathcal{P}_{22}) & 0 \\ 0 & 2i q \kappa_{Pf}^- \mathcal{P}_{11} & 2i q \kappa_{Ps}^- \mathcal{P}_{12} & (\kappa_S^{-2} + q^2) \\ 1 & \mathcal{A}_{4,2} & \mathcal{A}_{4,3} & 2i q \mu^- \kappa_S^- \end{bmatrix},$$

with

$$A_{4,2} = \frac{(\lambda^- + m^- \beta^{-2}) \mathcal{P}_{11} + m^- \beta^- \mathcal{P}_{21}}{V_{Pf}^{-2}} + 2\mu^- \kappa_{Pf}^{-2} \mathcal{P}_{11},$$

$$A_{4,3} = \frac{(\lambda^- + m^- \beta^{-2}) \mathcal{P}_{12} + m^- \beta^- \mathcal{P}_{22}}{V_{Ps}^{-2}} + 2\mu^- \kappa_{Ps}^{-2} \mathcal{P}_{12}.$$

Property 2.1. We easily check that $\mathcal{R}(-a + i b) = \overline{\mathcal{R}(a + i b)}$ and $\mathcal{T}_i(-a + i b) = \overline{\mathcal{T}_i(a + i b)}$.

4. Definition of the arrival time of the volume waves.

(a) For a given point (x, y) , we define the arrival time of the incident wave by

$$t_{\text{inc}}^{0+} = \frac{\sqrt{x^2 + (y - h)^2}}{V^+};$$

(b) for a given point (x, y) , we define t_{ref}^{0+} the arrival time of the reflected wave by

$$t_{\text{ref}}^{0+} = \frac{\sqrt{x^2 + (y + h)^2}}{V^+};$$

(c) for the definition of the arrival time of the transmitted i wave ($i \in \{Pf, Ps, S\}$) t_i^{0-} , we first have to determine the fastest path from the source to the point (x, y) : we search a point ξ_0 on the interface between the two media which minimizes the function

$$t(\xi) = \frac{\sqrt{\xi^2 + h^2}}{V^+} + \frac{\sqrt{(x - \xi)^2 + y^2}}{V_i^-}$$

(see Fig. 3). This leads us to find ξ_0 such that

$$t'(\xi_0) = \frac{\xi_0}{V^+ \sqrt{\xi_0^2 + h^2}} + \frac{\xi_0 - x}{V_i^- \sqrt{(x - \xi_0)^2 + y^2}} = 0. \quad (14)$$

From a numerical point of view, the solution of this equation is done by computing the roots of the following fourth degree polynomial

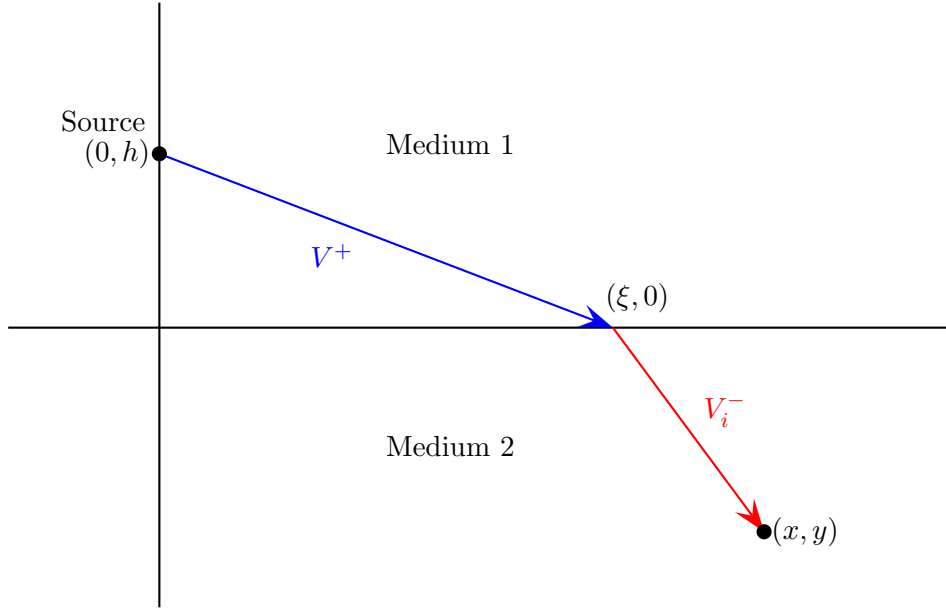
$$\left(\frac{1}{V^+} - \frac{1}{V_i^-} \right) X^4 + 2x \left(\frac{1}{V_i^-} - \frac{1}{V^+} \right) X^3 + \left(\frac{x^2 + y^2}{V^+} - \frac{x^2 + h^2}{V_i^-} \right) X^2 + \frac{xh^2}{V_i^-} X + \frac{x^2 h^2}{V_i^-},$$

ξ_0 is thus the only real root of this polynomial located between 0 and x which is also solution of (14). Once ξ_0 is computed, we can define

$$t_i^{0-} = \frac{\sqrt{\xi_0^2 + h^2}}{V^+} + \frac{\sqrt{(x - \xi_0)^2 + y^2}}{V_i^-}$$

5. Definition of the paths in the complex plane for the computation of the volume waves.

For computing the solution we'll use the following paths in the complex plane :

Figure 3: Path of the transmitted i wave

(a) For the reflected wave we define

$$\gamma^+(t) = -i \frac{x}{r^2} t + \frac{y+h}{r} \sqrt{\frac{t^2}{r^2} - \frac{1}{V^+}} \quad \text{for } t > \frac{r}{V^+}.$$

(b) For the transmitted waves, we first need to define the functions

$$\mathcal{F}_i^-(q, t) = -y \left(\frac{1}{V_i^-} + q^2 \right)^{\frac{1}{2}} + h \left(\frac{1}{V^+} + q^2 \right)^{\frac{1}{2}} + iqx - t$$

for $i \in \{Pf, Ps, S\}$. Before defining the paths in complex plane, let us recall some of the properties of the functions \mathcal{F}_i^- (see [4, 14, 7])

Property 2.2. *For each $t \in \mathbb{R}^+$, $\mathcal{F}_i^-(q, t_0)$ admits at most two roots.*

Property 2.3. *There is one and only one $t_0 \in \mathbb{R}^+$ such that $\mathcal{F}_i^-(q, t_0)$ admits a double root q_0 . This root is purely imaginary and t_0 corresponds to the arrival time of the wave: $t_0 = t_i^{0-}$. Moreover $\Im m(q_0) \leq 0$ if $x \geq 0$ and $\Im m(q_0) > 0$ if $x < 0$*

Property 2.4. *For $t > t_i^{0+}$, $\mathcal{F}_i^-(q, t)$, admits exactly two roots, which have the same imaginary part and an opposite non-zero real part.*

We are now able to define the path $\gamma_i^-(t)$ for $t > t_i^{0-}$ as the only root of $\mathcal{F}_i^-(q, t)$ whose real part is positive. From a numerical point of view, we won't directly compute the roots of $\mathcal{F}_i^-(q, t)$ but we will derive a polynomial F of fourth degree from it such that the roots of $\mathcal{F}_i^-(q, t)$ are also roots of F . $\gamma_i^-(t)$ will be the only common root of F and $\mathcal{F}_i^-(q, t)$ with a positive real part.

Remark 2.2. The derivative of $\gamma_i^-(t)$ can be easily computed thanks to the implicit function theorem :

$$\frac{d\gamma_i^-(t)}{dt} = -y \frac{\gamma_i^-(t)}{\left(\frac{1}{V_i^{-2}} + \gamma_i^{-2}(t)\right)^{\frac{1}{2}}} + h \frac{\gamma_i^-(t)}{\left(\frac{1}{V^+2} + \gamma_i^{-2}(t)\right)^{\frac{1}{2}}} + i x$$

Since $\mathcal{F}_i^-(q, t)$ admits a double root at $t = t_i^{0-}$, the functions $\frac{d\gamma_i^-(t)}{dt}$ are singular at this point, however this singularity behaves as [7]

$$\frac{\alpha}{\sqrt{t^2 - t_i^{0-2}}}$$

and can therefore be integrated.

Remark 2.3. For the reflected wave, the path $\gamma^+(t)$ is actually the root of the function

$$\mathcal{F}^+(q, t) = (y + h) \left(\frac{1}{V^+} + q^2 \right)^{\frac{1}{2}} + i q x - t$$

6. Definition of the arrival time of the head waves.

- **For the reflected wave** ($y \geq 0$). There are two conditions for the arrival of a reflected head wave at point (x, y)
 - The velocity V^+ must not be greater than all the velocities in the bottom medium: $V^+ < V_{\max}$ with

$$V_{\max} = \max(V_i^-)_{i \in \{Pf, Ps, S\}}.$$

- The point (x, y) must satisfy the relation

$$\frac{|x|}{\sqrt{x^2 + (y + h)^2}} > \frac{V^+}{V_{\max}}$$

If these two conditions are realized, t^{h+} , the arrival time of the reflected head wave is such that $|\gamma^+(t^{h+})| = \frac{1}{V_{\max}}$. It is easily obtained by choosing $q = \frac{-i}{V_{\max}}$ (if $x > 0$) or $q = \frac{i}{V_{\max}}$ (if $x < 0$) in the expression of $\mathcal{F}^+(q, t)$:

$$t^{h+} = y \sqrt{\frac{1}{V^+2} - \frac{1}{V_{\max}^2}} + h \sqrt{\frac{1}{V^+2} - \frac{1}{V_{\max}^2}} + \frac{|x|}{V_{\max}}$$

- **For a transmitted wave** ($y < 0$). There are two conditions for the arrival of a transmitted head wave i at point (x, y) :
 - The velocity V_i^- must not be greater than all the other velocities in the bottom medium: $V_i^- < V_{\max}$ with

$$V_{\max} = \max(V_j^-)_{j \in \{Pf, Ps, S\}, j \neq i}$$

- (b) The double root of $\mathcal{F}_i^-(q, t_i^{0-})$ must be lying on the branch cut of one function κ_j^- :

$$|\gamma_i^-(t_i^{0-})| > \frac{1}{V_{\max}}.$$

If these two conditions are realized, t_i^{h-} , the arrival time of the transmitted head wave i is such that $|\gamma_i^-(t_i^{h-})| = \frac{1}{V_{\max}}$. It is easily obtained by choosing $q = \frac{-i}{V_{\max}}$ (if $x > 0$) or $q = \frac{i}{V_{\max}}$ (if $x < 0$) in the expression of $\mathcal{F}_i^-(q, t)$:

$$t_i^{h-} = -y \sqrt{\frac{1}{V_i^{-2}} - \frac{1}{V_{\max}^2}} + h \sqrt{\frac{1}{V^+{}^2} - \frac{1}{V_{\max}^2}} + \frac{|x|}{V_{\max}}$$

7. Definition of the paths in the complex plane for the computation of the head waves.

For computing the solution we'll use the following paths in the complex plane :

- (a) For the reflected wave we define

$$\begin{cases} v^+(t) = -i \left(\frac{y+h}{r} \sqrt{\frac{1}{V^+} \frac{t^2}{r^2}} + \frac{x}{r^2} t \right) & \text{if } t^{h+} < t \leq t^{0+} \text{ and } x < 0 \\ v^+(t) = i \left(\frac{y+h}{r} \sqrt{\frac{1}{V^+} - \frac{t^2}{r^2}} - \frac{x}{r^2} t \right) & \text{if } t^{h+} < t \leq t^{0+} \text{ and } x \geq 0 \end{cases}$$

- (b) For the transmitted waves, we'll use once again the functions $\mathcal{F}_i^-(q, t)$ after having recalled the following properties:

Property 2.5. For $t_i^{h-} < t \leq t_i^{0-}$, the function $\mathcal{F}_i^-(q, t)$ admits exactly two imaginary roots $q_1(t)$ and $q_2(t)$ such that

$$\Im m(q_1(t)) \in [\Im m(\gamma_i^-(t_i^{0-})), 1/V_{\max}] \text{ and } \Im m(\partial_t q_1(t)) < 0$$

$$\Im m(q_2(t)) \in [-1/V_{\max}, \Im m(\gamma_i^-(t_i^{0-}))] \text{ and } \Im m(\partial_t q_2(t)) > 0$$

If $x \geq 0$, $\Im m(\gamma_i^-(t_i^{0-})) \leq 0$ (property 2.3), so that $\gamma_i^-(t_i^{0-})$ lies on the branch cut

$$\left\{ q \in \mathbb{C} \mid \Re e(q) = 0 \text{ and } \Im m(q) < -\frac{1}{V_{\max}} \right\}.$$

Therefore we need the path $q_2(t)$ to bypass the branch cut and we define

$$\Im m \left(\frac{dv_i^-(t)}{dt} \right) = \Im m \left(-y \frac{v_i^-(t)}{\left(\frac{1}{V_i^{-2}} + v_i^{-2}(t) \right)^{\frac{1}{2}}} + h \frac{v_i^-(t)}{\left(\frac{1}{V^+{}^2} + v_i^{-2}(t) \right)^{\frac{1}{2}}} + ix \right) < 0.$$

If $x < 0$, we need the path $q_1(t)$ to bypass the branch cut and we define

$$\Im m \left(\frac{dv_i^-(t)}{dt} \right) = \Im m \left(-y \frac{v_i^-(t)}{\left(\frac{1}{V_i^{-2}} + v_i^{-2}(t) \right)^{\frac{1}{2}}} + h \frac{v_i^-(t)}{\left(\frac{1}{V^+{}^2} + v_i^{-2}(t) \right)^{\frac{1}{2}}} + ix \right) > 0.$$

2.2 Main result

Theorem 2.1. *The pressure and the displacement in the top medium are given by*

$$p^+(x, y, t) = p_{inc}^+(x, y, t) + p_{ref}^+(x, y, t) \text{ and } \mathbf{u}^+(x, y, t) = \int_0^t \nu_{inc}^+(x, y, \tau) d\tau + \int_0^t \nu_{ref}^+(x, y, \tau) d\tau,$$

the displacement in the bottom medium is given by

$$\mathbf{u}_s^- = \int_0^t \nu^-(x, y, \tau) d\tau \text{ with } \nu^- = \nu_{Pf}^- + \nu_{Ps}^- + \nu_S^-,$$

where

- $p_{inc}^+(x, y, t)$ and $\nu_{inc}^+(x, y, t)$ correspond to the incident wave and satisfy :

$$\begin{cases} p_{inc}^+(x, y, t) = \frac{1}{2\pi\sqrt{t^2 - \frac{r^2}{V^{+2}}}}, & \text{if } t > t_{inc}^{0+}, \\ p_{inc}^+(x, y, t) = 0, & \text{else.} \end{cases},$$

$$\begin{cases} \nu_{inc,x}(x, y, t) = \frac{tx}{2\pi\rho^+ r \sqrt{t^2 - \frac{r^2}{V^{+2}}}}, & \text{if } t > t_{inc}^{0+}, \\ \nu_{inc,x}(x, y, t) = 0, & \text{else.} \end{cases}$$

and

$$\begin{cases} \nu_{inc,y}(x, y, t) = \frac{t(y-h)}{2\pi\rho^+ r \sqrt{t^2 - \frac{r^2}{V^{+2}}}}, & \text{if } t > t_{inc}^{0+}, \\ \nu_{inc,y}(x, y, t) = 0, & \text{else} \end{cases}$$

with $r = \sqrt{x^2 + (y-h)^2}$.

- $p_{ref}^+(x, y, t)$ and $\nu_{ref}^+(x, y, t)$ correspond to the reflected wave and satisfy :

$$\begin{cases} p_{ref}^+(x, y, t) = -\frac{\Im m(\kappa^+(\nu^+(t))\mathcal{R}(\nu^+(t)))}{\pi\sqrt{\frac{r^2}{V^{+2}} - t^2}}, & \text{if } t^{h+} < t \leq t_{ref}^{0+} \text{ and } \frac{x}{r} > \frac{V^+}{V_{\max}} \\ p_{ref}^+(x, y, t) = \frac{\Re e(\kappa^+(\gamma^+(t))\mathcal{R}(\gamma^+(t)))}{\pi\sqrt{\frac{r^2}{V^{+2}} - t^2}}, & \text{if } t > t_{ref}^{0+} \\ p_{ref}^+(x, y, t) = 0, & \text{else,} \end{cases}$$

$$\begin{cases} \nu_{ref,x}^+(x, y, t) = \frac{\Im m(i\nu^+(t)\kappa^+(\nu^+(t))\mathcal{R}(\nu^+(t)))}{\pi\rho^+\sqrt{\frac{r^2}{V^{+2}} - t^2}}, & \text{if } t^{h+} < t \leq t_{ref}^{0+} \text{ and } \frac{x}{r} > \frac{V^+}{V_{\max}} \\ \nu_{ref,x}^+(x, y, t) = -\frac{\Re e(i\gamma^+(t)\kappa^+(\gamma^+(t))\mathcal{R}(\gamma^+(t)))}{\pi\rho^+\sqrt{\frac{r^2}{V^{+2}} - t^2}}, & \text{if } t > t_{ref}^{0+} \\ \nu_{ref,x}^+(x, y, t) = 0, & \text{else} \end{cases}$$

and

$$\begin{cases} \nu_{ref,y}^+(x, y, t) = -\frac{\Im m \left(\kappa^{+2}(v^+(t)) \mathcal{R}(v^+(t)) \right)}{\pi \rho^+ \sqrt{t^2 - \frac{r^2}{V^{+2}}}}, & \text{if } t^{h+} < t \leq t_{ref}^{0+} \text{ and } \frac{x}{r} > \frac{V^+}{V_{\max}}, \\ \nu_{ref,y}^+(x, y, t) = \frac{\Re e \left(\kappa^{+2}(\gamma^+(t)) \mathcal{R}(\gamma^+(t)) \right)}{\pi \rho^+ \sqrt{t^2 - \frac{r^2}{V^{+2}}}}, & \text{if } t > t_{ref}^{0+} \\ \nu_{ref,y}^+(x, y, t) = 0, & \text{else} \end{cases}$$

with $r = \sqrt{x^2 + (y + h)^2}$ and $V_{\max} = \max(V_{Pf}, V_{Ps}, V_S)$.

- $\nu_{Pf}^-(x, y, t)$ corresponds to the transmitted Pf wave and satisfies:

$$\begin{cases} \nu_{Pf,x}^-(x, y, t) = \frac{\mathcal{P}_{11}}{\pi} \Re e \left(i v_{Pf}^-(t) \mathcal{T}_{Pf}(v_{Pf}^-(t)) \frac{dv_{Pf}^-}{dt}(t) \right), & \text{if } t_{Pf}^{h-} < t \leq t_{Pf}^{0-} \text{ and } |\Im m(v_{Pf}^-(t_{Pf}^{0-}))| > \frac{1}{V_{\max}}, \\ \nu_{Pf,x}^-(x, y, t) = \frac{\mathcal{P}_{11}}{\pi} \Re e \left(i \gamma_{Pf}^-(t) \mathcal{T}_{Pf}(\gamma_{Pf}^-(t)) \frac{d\gamma_{Pf}^-}{dt}(t) \right), & \text{if } t > t_{Pf}^{0-}, \\ \nu_{Pf,x}^-(x, y, t) = 0, & \text{else} \end{cases}$$

and

$$\begin{cases} \nu_{Pf,y}^-(x, y, t) = \frac{\mathcal{P}_{11}}{\pi} \Re e \left(\kappa_{Pf}^-(v_{Pf}^-(t)) \mathcal{T}_{Pf}(v_{Pf}^-(t)) \frac{dv_{Pf}^-}{dt}(t) \right), & \text{if } t_{Pf}^{h-} < t \leq t_{Pf}^{0-} \text{ and } |\Im m(v_{Pf}^-(t_{Pf}^{0-}))| > \frac{1}{V_{\max}}, \\ \nu_{Pf,y}^-(x, y, t) = \frac{\mathcal{P}_{11}}{\pi} \Re e \left(\kappa_{Pf}^-(\gamma_{Pf}^-(t)) \mathcal{T}_{Pf}(\gamma_{Pf}^-(t)) \frac{d\gamma_{Pf}^-}{dt}(t) \right), & \text{if } t > t_{Pf}^{0-}, \\ \nu_{Pf,y}^-(x, y, t) = 0, & \text{else} \end{cases}$$

with $V_{\max} = \max(V_{Ps}, V_S)$.

- $\nu_{Ps}^-(x, y, t)$ corresponds to the transmitted Ps wave and satisfies:

$$\begin{cases} \nu_{Ps,x}^-(x, y, t) = \frac{\mathcal{P}_{12}}{\pi} \Re e \left(i v_{Ps}^-(t) \mathcal{T}_{Ps}(v_{Ps}^-(t)) \frac{dv_{Ps}^-}{dt}(t) \right), & \text{if } t_{Ps}^{h-} < t \leq t_{Ps}^{0-} \text{ and } |\Im m(v_{Ps}^-(t_{Ps}^{0-}))| > \frac{1}{V_{\max}}, \\ \nu_{Ps,x}^-(x, y, t) = \frac{\mathcal{P}_{12}}{\pi} \Re e \left(i \gamma_{Ps}^-(t) \mathcal{T}_{Ps}(\gamma_{Ps}^-(t)) \frac{d\gamma_{Ps}^-}{dt}(t) \right), & \text{if } t > t_{Ps}^{0-}, \\ \nu_{Ps,x}^-(x, y, t) = 0, & \text{else} \end{cases}$$

and

$$\left\{ \begin{array}{ll} \nu_{P_s,y}^-(x,y,t) = \frac{\mathcal{P}_{12}}{\pi} \Re e \left(\kappa_{P_s}^-(v_{P_s}^-(t)) \mathcal{T}_{P_s}(v_{P_s}^-(t)) \frac{dv_{P_s}^-}{dt}(t) \right), & \text{if } t_{P_s}^{h-} < t \leq t_{P_s}^{0-} \\ & \text{and } |\Im m(v_{P_s}^-(t_{P_s}^{0-}))| > \frac{1}{V_{\max}}, \\ \nu_{P_s,y}^-(x,y,t) = \frac{\mathcal{P}_{12}}{\pi} \Re e \left(\kappa_{P_s}^-(\gamma_{P_s}^-(t)) \mathcal{T}_{P_s}(\gamma_{P_s}^-(t)) \frac{d\gamma_{P_s}^-}{dt}(t) \right), & \text{if } t > t_{P_s}^{0-}, \\ \nu_{P_s,y}^-(x,y,t) = 0, & \text{else} \end{array} \right.$$

with $V_{\max} = \max(V_{P_f}, V_S)$.

- $\nu_S^-(x,y,t)$ corresponds to the transmitted S wave and satisfies:

$$\left\{ \begin{array}{ll} \nu_{S,x}^-(x,y,t) = \frac{1}{\pi} \Re e \left(\kappa_S^-(v_S^-(t)) \mathcal{T}_S(v_S^-(t)) \frac{dv_S^-}{dt}(t) \right), & \text{if } t_S^{h-} < t \leq t_S^{0-} \\ & \text{and } |\Im m(v_S^-(t_S^{0-}))| > \frac{1}{V_{\max}}, \\ \nu_{S,x}^-(x,y,t) = \frac{1}{\pi} \Re e \left(\kappa_S^-(\gamma_S^-(t)) \mathcal{T}_S(\gamma_S^-(t)) \frac{d\gamma_S^-}{dt}(t) \right), & \text{if } t > t_S^{0-}, \\ \nu_{S,x}^-(x,y,t) = 0, & \text{else} \end{array} \right.$$

and

$$\left\{ \begin{array}{ll} \nu_{S,y}^-(x,y,t) = -\frac{1}{\pi} \Re e \left(i v_S^-(t) \mathcal{T}_S(v_S^-(t)) \frac{dv_S^-}{dt}(t) \right), & \text{if } t_S^{h-} < t \leq t_S^{0-} \\ & \text{and } |\Im m(v_S^-(t_S^{0-}))| > \frac{1}{V_{\max}}, \\ \nu_{S,y}^-(x,y,t) = -\frac{1}{\pi} \Re e \left(i \gamma_S^-(t) \mathcal{T}_S(\gamma_S^-(t)) \frac{d\gamma_S^-}{dt}(t) \right), & \text{if } t > t_S^{0-}, \\ \nu_{S,y}^-(x,y,t) = 0, & \text{else} \end{array} \right.$$

with $V_{\max} = \max(V_{P_f}, V_{P_s})$.

Remark 2.4. For the practical computations, we won't have to explicitly compute the primitive of the functions ν , which would be rather tedious, since

$$\left(\int_0^t \nu(\tau) d\tau \right) * f = \nu * \left(\int_0^t f(\tau) d\tau \right).$$

Therefore, we'll only have to compute the primitive of the source function f .

2.3 Proof of the theorem

Let us first apply a Laplace transform in time

$$\tilde{u}(x,y,s) = \int_0^{+\infty} u(x,y,t) e^{-st} dt,$$

and a Fourier transform in the x variable

$$\hat{u}(k_x, y, s) = \int_{-\infty}^{+\infty} \tilde{u}(x, y, s) e^{ik_x x} dx.$$

to (12) we obtain

$$\begin{cases} \left(\frac{s^2}{V^{+2}} + k_x^2 \right) \hat{p}^+ - \frac{\partial^2 \hat{p}^+}{\partial y^2} = \frac{\delta(y-h)}{V^{+2}}, & y > 0, \\ \left(\frac{s^2}{V_i^{-2}} + k_x^2 \right) \hat{\Phi}_i^- - \frac{\partial^2 \hat{\Phi}_i^-}{\partial y^2} = 0, \quad i \in \{Pf, Ps, S\} & y < 0, \\ \hat{\mathcal{B}}(\hat{p}^+, \hat{\Phi}_{Pf}^-, \hat{\Phi}_{Ps}^-, \hat{\Phi}_S^-) = 0 & y = 0. \end{cases} \quad (15)$$

Where $\hat{\mathcal{B}}$ is the Laplace-Fourier transform of the operator \mathcal{B} .

From the two first equations of (15), we deduce that the solution $(\hat{p}^+, (\hat{\Phi}_i^-)_{i \in \{Pf, Ps, S\}})$ is such that

$$\begin{cases} \hat{p}^+ = \hat{p}_{\text{inc}}^+ + \hat{p}_{\text{ref}}^+, \\ \hat{p}_{\text{inc}}^+ = \frac{1}{s\kappa^+(\frac{k_x}{s})} e^{-s|y-h|\kappa^+(\frac{k_x}{s})}, \hat{p}_{\text{ref}}^+ = R(k_x, s) e^{-sy\kappa^+(\frac{k_x}{s})}, \\ \hat{\Phi}_i^- = T_i(k_x, s) e^{-s(y\kappa_i^-(\frac{k_x}{s}))}, \quad i \in \{Pf, Ps, S\}, \end{cases} \quad (16)$$

and, using the last equation of (15), we obtain

$$\hat{\mathcal{B}}(\hat{p}_{\text{ref}}^+, \hat{\Phi}_{Pf}^-, \hat{\Phi}_{Ps}^-, \hat{\Phi}_S^-) = -\hat{\mathcal{B}}(\hat{p}_{\text{inc}}^+, 0, 0, 0)$$

for $y = 0$, or, from (16):

$$\hat{\mathcal{B}}(R(k_x, s), T_{Pf}(k_x, s), T_{Ps}(k_x, s), T_S(k_x, s)) = -\hat{\mathcal{B}}\left(\frac{e^{-sh\kappa^+(\frac{k_x}{s})}}{s\kappa^+(\frac{k_x}{s})}, 0, 0, 0\right).$$

After some calculations that we don't detail here, we obtain that $(R(k_x, s), T_{Pf}(k_x, s), T_{Ps}(k_x, s), T_S(k_x, s))$ is solution of

$$\mathcal{A}\left(\frac{k_x}{s}\right) \begin{bmatrix} R(k_x, s) \\ s^2 T_{Pf}(k_x, s) \\ s^2 T_{Ps}(k_x, s) \\ s^2 T_S(k_x, s) \end{bmatrix} = -\frac{e^{-sh\kappa^+(\frac{k_x}{s})}}{2s\kappa^+(\frac{k_x}{s}) V^{+2}} \begin{bmatrix} \frac{\kappa^+(\frac{k_x}{s})}{\rho^+} \\ 1 \\ 0 \\ 1 \end{bmatrix}. \quad (17)$$

From the definition of the reflection and transmission coefficient given at § 2.1, we deduce that

$$\begin{bmatrix} R(k_x, s) \\ s^2 T_{Pf}(k_x, s) \\ s^2 T_{Ps}(k_x, s) \\ s^2 T_S(k_x, s) \end{bmatrix} = \frac{1}{s} \begin{bmatrix} \mathcal{R}\left(\frac{k_x}{s}\right) \\ T_{Pf}\left(\frac{k_x}{s}\right) \\ T_{Ps}\left(\frac{k_x}{s}\right) \\ T_S\left(\frac{k_x}{s}\right) \end{bmatrix} e^{-sh\kappa^+(\frac{k_x}{s})}. \quad (18)$$

Finally:

$$\begin{cases} \hat{p}^+ = \hat{p}_{\text{inc}}^+ + \hat{p}_{\text{ref}}^+, \\ \hat{p}_{\text{inc}}^+ = \frac{1}{s\kappa^+(\frac{k_x}{s})} e^{-s|y-h|\kappa^+(\frac{k_x}{s})}, \hat{p}_{\text{ref}}^+ = \frac{1}{s} \mathcal{R}\left(\frac{k_x}{s}\right) e^{-s(y+h)\kappa^+(\frac{k_x}{s})}, \\ \hat{\Phi}_i^- = \frac{1}{s^3} \mathcal{T}_i\left(\frac{k_x}{s}\right) e^{-s(y\kappa_i^-(\frac{k_x}{s}) - h\kappa^+(\frac{k_x}{s}))}, \quad i \in \{Pf, Ps, S\}, \end{cases} \quad (19)$$

and

$$\begin{cases} \hat{u}^+ = \hat{u}_{\text{inc}}^+ + \hat{u}_{\text{ref}}^+, \\ \hat{u}_{\text{inc},x}^+ = -i \frac{k_x}{\rho^+ s^2} \hat{p}_{\text{inc}}^+, \quad \hat{u}_{\text{inc},y}^+ = \text{sign}(h-y) \frac{\kappa^+(\frac{k_x}{s})}{\rho^+ s} \hat{p}_{\text{inc}}^+, \\ \hat{u}_{\text{ref},x}^+ = -i \frac{k_x}{\rho^+ s^2} \hat{p}_{\text{ref}}^+, \quad \hat{u}_{\text{ref},y}^+ = \frac{\kappa^+(\frac{k_x}{s})}{\rho^+ s} \hat{p}_{\text{ref}}^+, \\ \hat{u}_{sx}^- = i k_x \mathcal{P}_{11} \hat{\Phi}_{Pf} + i k_x \mathcal{P}_{12} \hat{\Phi}_{Ps}^- + s \kappa_S^-\left(\frac{k_x}{s}\right) \Phi_S^-, \\ \hat{u}_{sy}^- = s \kappa_{Pf}^-\left(\frac{k_x}{s}\right) \mathcal{P}_{11} \hat{\Phi}_{Pf}^- + s \kappa_{Ps}^-\left(\frac{k_x}{s}\right) \mathcal{P}_{12} \hat{\Phi}_{Ps}^- - i k_x \Phi_S^- \end{cases} \quad (20)$$

The rest of the proof is a direct application of the Cagniard-de Hoop method (see [4, 6, 14, 13, 11, 7, 9]) and we only detail the computation of $\hat{u}_{sx,Ps}^- = i k_x \mathcal{P}_{12} \hat{\Phi}_s^-$, since the other ones are very similar. We define $V_{\max} = \max(V_{Pf}, V_S)$, since $V_{Ps} < V_{Pf}$ it is clear that $V_{Ps} < V_{\max}$. We apply an inverse Fourier transform in the x variable to $\hat{u}_{sx,Ps}^-$ and we set $k_x = qs$ to obtain

$$\tilde{u}_{sx,Ps}^- = \int_{-\infty}^{+\infty} \frac{i q \mathcal{P}_{12}}{2s\pi} \mathcal{T}_{Ps}(q) e^{-s(-y\kappa_{Ps}^-(q) + h\kappa^+(q) + iqx)} dq = \frac{\mathcal{P}_{12}}{2s\pi} \int_{-\infty}^{+\infty} \Xi(q) dq. \quad (21a)$$

We now have to define a path in the complex plane, so that $(-y\kappa_{Ps}^-(q) + h\kappa^+(q) + iqx) = t \in \mathbb{R}^+$, this can be easily done thanks to the function $\gamma_{Ps}^-(t)$. Therefore we define

$$\Gamma_R^+ = \{\gamma_{Ps}^-(t) \mid t_{Ps}^{0-} < t < R\} \text{ and } \Gamma_R^- = \left\{ -\overline{\gamma_{Ps}^-(t)} \mid t_{Ps}^{0-} < t < R \right\}.$$

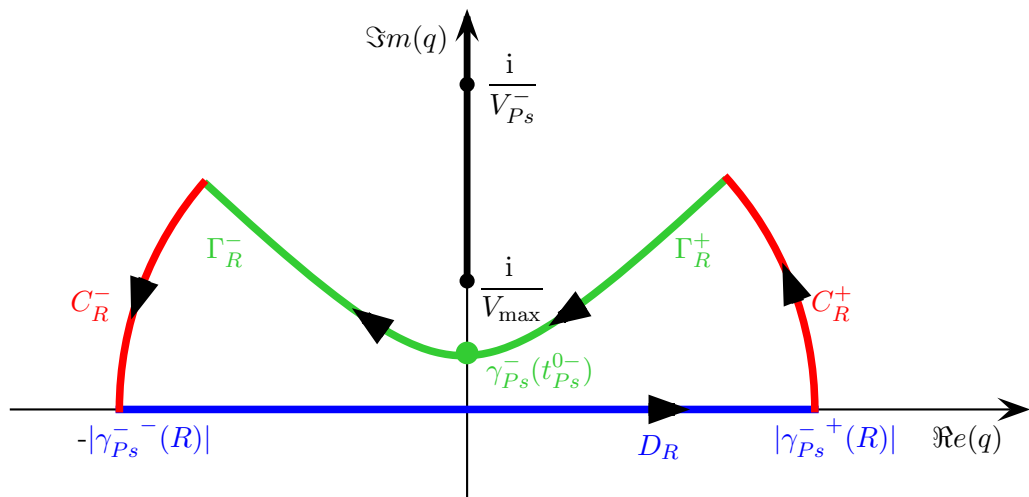
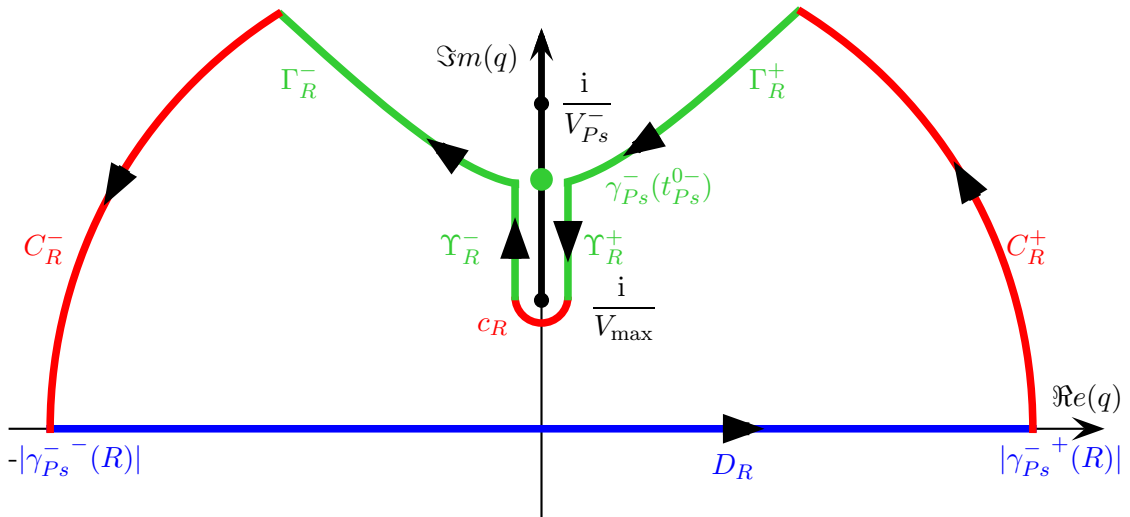
We represent the path $\Gamma_R = \Gamma_R^+ \cup \Gamma_R^-$ in Figs. 5 and 4 for $x < 0$ (for $x \geq 0$ the path would be similar but in the half plane $\Im m(q) \leq 0$). We denote by D_R the real segment $[-|\gamma_{Ps}^-(R)|; |\gamma_{Ps}^-(R)|]$. As shown in the two figures, we have to consider two possibilities:

- if $|\gamma_{Ps}^-(t_{Ps}^{0-})| > \frac{1}{V_{\max}}$ (Fig.4), then Γ_R does not intersect the branch cuts of the functions κ_i^- or κ^+ and we close the path by the two arcs of circle C_R^- and C_R^+ represented on Fig.4. By Cauchy's theorem :

$$\int_{D_R} \Xi(q) dq + \int_{C_R^+} \Xi(q) dq + \int_{\Gamma_R} \Xi(q) dq + \int_{C_R^-} \Xi(q) dq = 0.$$

Moreover, by using Jordan's lemma, we have:

$$\lim_{R \rightarrow \infty} \int_{C_R^\pm} \Xi(q) dq = 0,$$

Figure 4: Integration path if $|\gamma_{Ps}^-(t_{Ps}^{0-})| < 1/V_{\max}$.Figure 5: Integration path if $|\gamma_{Ps}^-(t_{Ps}^{0-})| > 1/V_{\max}$.

then

$$\int_{-\infty}^{+\infty} \Xi(q) dq = - \int_{\Gamma_{+\infty}} \Xi(q) dq = - \int_{\Gamma_{+\infty}^+} \Xi(q) dq - \int_{\Gamma_{+\infty}^-} \Xi(q) dq.$$

Let us now use the change of variable $q = -\overline{\gamma_{Ps}^-(t)}$ on $\Gamma_{+\infty}^-$ and $q = \gamma_{Ps}^-(t)$ on $\Gamma_{+\infty}^+$:

$$\int_{-\infty}^{+\infty} \Xi(q) dq = \int_{t_{Ps}^{0,+}}^{\infty} i \gamma_{Ps}^-(t) \mathcal{T}_{Ps}(\gamma_{Ps}^-(t)) \frac{d\gamma_s^-(t)}{dt} e^{-st} dt - \int_{t_{Ps}^{0,+}}^{\infty} i \overline{\gamma_{Ps}^-(t)} \mathcal{T}_{Ps}(-\overline{\gamma_{Ps}^-(t)}) \overline{\frac{d\gamma_s^-(t)}{dt}} e^{-st} dt.$$

From the property 2.1 we deduce $\mathcal{T}_{Ps}(\overline{\gamma_{Ps}^-(t)}) = \overline{\mathcal{T}_{Ps}(\gamma_{Ps}^-(t))}$ and

$$i \overline{\gamma_{Ps}^-(t)} \mathcal{T}_{Ps}(-\overline{\gamma_{Ps}^-(t)}) \overline{\frac{d\gamma_s^-(t)}{dt}} = -i \gamma_{Ps}^-(t) \mathcal{T}_{Ps}(\gamma_{Ps}^-(t)) \frac{d\gamma_s^-(t)}{dt}.$$

Then

$$\begin{aligned} \tilde{u}_{sx,Ps}^-(x, y, s) &= \int_{t_{Ps}^{0,-}}^{\infty} \frac{\mathcal{P}_{12}}{s\pi} \Re e \left(i \gamma_{Ps}^-(t) \mathcal{T}_{Ps}(\gamma_{Ps}^-(t)) \frac{d\gamma_s^-(t)}{dt} \right) e^{-st} dt \\ &= \int_{t_{Ps}^{0,-}}^{\infty} \left[\int_0^t \nu_{s,x}^-(x, y, \tau) d\tau \right] e^{-st} dt. \end{aligned}$$

We conclude by using the injectivity of the Laplace transform that

$$u_{sx,Ps}^-(x, y, t) = \int_0^t \nu_{s,x}^-(x, y, \tau) d\tau, \text{ for } t \geq t_{Ps}^{0,-}$$

- if $|\gamma_{Ps}^-(t_{Ps}^{0,-})| < \frac{1}{V_{\max}}$ (Fig.5), then Γ_R intersects the branch cuts of (at least) one function $(\kappa_i^-)_{i \in \{Fp,S\}}$ and we have to bypass it thanks to the paths

$$\Upsilon_R = \Upsilon_R^+ \cup \Upsilon_R^- \text{ with } \Upsilon_R^\pm = \left\{ v_{Ps}^-(t) \pm \frac{1}{R} \mid t_{Ps}^{h-} < t < t_{Ps}^{0-} \right\}$$

(see Fig.5) and we close the path by the three arcs of circle C_R^- , C_R^+ and c_R represented on Fig.5. By Cauchy's theorem :

$$\int_{D_R} \Xi(q) dq + \int_{C_R^+} \Xi(q) dq + \int_{\Gamma_R} \Xi(q) dq + \int_{\Upsilon_R} \Xi(q) dq + \int_{C_R^-} \Xi(q) dq + \int_{c_R} \Xi(q) dq = 0.$$

Using once again Jordan's Lemma, we prove that the integrals over C_R^- , C_R^+ and c_R vanish when R tends to infinity and that

$$\int_{-\infty}^{+\infty} \Xi(q) dq = - \int_{\Gamma_{+\infty}} \Xi(q) dq - \int_{\Upsilon_{+\infty}} \Xi(q) dq.$$

The calculation of the integral over $\Gamma_{+\infty}$ is done as in the first case and we only focus on the calculation over $\Upsilon_{+\infty}$:

$$\int_{\Upsilon_{+\infty}} \Xi(q) dq = \int_{\Upsilon_{+\infty}^-} \Xi(q) dq + \int_{\Upsilon_{+\infty}^+} \Xi(q) dq$$

Let us now use the change of variable $q = v_{Ps}^-(t) - 1/R$ on Υ_R^- and $q = v_{Ps}^-(t) + 1/R$ on Υ_R^+ :

$$\begin{aligned}\int_{\Upsilon_R} \Xi(q) dq &= \int_{t_{Ps}^{h-}}^{t_{Ps}^{0-}} i \left(v_{Ps}^-(t) - \frac{1}{R} \right) \mathcal{T}_{Ps} \left(v_{Ps}^-(t) - \frac{1}{R} \right) \frac{dv_{Ps}^-(t)}{dt} e^{-st} dt \\ &\quad - \int_{t_{Ps}^{h-}}^{t_{Ps}^{0-}} i \left(v_{Ps}^-(t) + \frac{1}{R} \right) \mathcal{T}_{Ps} \left(v_{Ps}^-(t) + \frac{1}{R} \right) \frac{dv_{Ps}^-(t)}{dt} e^{-st} dt.\end{aligned}$$

Because of the branch cut, it is clear that

$$\lim_{R \rightarrow +\infty} \mathcal{T}_{Ps}(v_{Ps}^-(t) + 1/R) \neq \lim_{R \rightarrow +\infty} \mathcal{T}_{Ps}(v_{Ps}^-(t) - 1/R),$$

however, from the property 2.1 we deduce $\mathcal{T}_{Ps}(v_{Ps}^-(t) - 1/R) = \overline{\mathcal{T}_{Ps}(v_{Ps}^-(t) + 1/R)}$ and following the definition of the square root of a negative number given at sec. 2.1, we'll make the notation abuse

$$\lim_{R \rightarrow +\infty} \mathcal{T}_{Ps}(v_{Ps}^-(t) + 1/R) = \mathcal{T}_{Ps}(v_{Ps}^-(t))$$

to obtain

$$\int_{\Upsilon_{+\infty}} \Xi(q) dq = \int_{t_{Ps}^{h-}}^{t_{Ps}^{0-}} 2v_{Ps}^-(t) \Im m(\mathcal{T}_{Ps}(v_{Ps}^-(t))) \frac{dv_{Ps}^-(t)}{dt} e^{-st} dt,$$

or, since $v_{Ps}^-(t)$ and $\frac{dv_{Ps}^-(t)}{dt}$ are purely imaginary:

$$\int_{\Upsilon_{+\infty}} \Xi(q) dq = - \int_{t_{Ps}^{h-}}^{t_{Ps}^{0-}} 2\Re e \left(i v_{Ps}^-(t) \mathcal{T}_{Ps}(v_{Ps}^-(t)) \frac{dv_{Ps}^-(t)}{dt} \right) e^{-st} dt,$$

Finally we have

$$\begin{aligned}\tilde{u}_{sx,Ps}^-(x, y, s) &= \int_{t_{Ps}^{h-}}^{t_{Ps}^{0-}} \frac{\mathcal{P}_{12}}{s\pi} \Re e \left(i v_{Ps}^-(t) \mathcal{T}_{Ps}(v_{Ps}^-(t)) \frac{dv_{Ps}^-(t)}{dt} \right) e^{-st} dt \\ &\quad + \int_{t_{Ps}^{0-}}^{\infty} \frac{\mathcal{P}_{12}}{s\pi} \Re e \left(i \gamma_{Ps}^-(t) \mathcal{T}_{Ps}(\gamma_{Ps}^-(t)) \frac{d\gamma_{Ps}^-(t)}{dt} \right) e^{-st} dt \\ &= \int_{t_{Ps}^{h-}}^{\infty} \left[\int_0^t \nu_{Ps,x}^-(x, y, \tau) d\tau \right] e^{-st} dt\end{aligned}$$

and we conclude by using the injectivity of the Laplace transform that

$$u_{sx,Ps}^-(x, y, t) = \int_0^t \nu_{Ps,x}^-(x, y, \tau) d\tau, \text{ for } t \geq t_{Ps}^{h-}$$

3 Comparison with a numerical solution

In order to validate our analytical solution, we have compared it to a numerical one obtained by C. Morency and J. Tromp [12]. We consider an acoustic layer with a density $\rho^+ = 1020 \text{ kg/m}^3$ and a celerity $V^+ = 1500 \text{ m/s}$ on top of a poroelastic layer whose characteristic coefficients are:

- the solid density $\rho_s^- = 2500 \text{ kg/m}^3$;
- the fluid density $\rho_f^- = 1020 \text{ kg/m}^3$;
- the porosity $\phi^- = 0.4$;
- the tortuosity $a^- = 2$;
- the solid bulk modulus $K_s^- = 16.0554 \text{ GPa}$;
- the fluid bulk modulus $K_f^- = 2.295 \text{ GPa}$;
- the frame bulk modulus $K_b^- = 10 \text{ GPa}$;
- the frame shear modulus $\mu^- = 9.63342 \text{ GPa}$;

so that the celerity of the waves in the poroelastic medium are:

- for the fast P wave, $V_{Pf} = 3677 \text{ m/s}$
- for the slow P wave, $V_{Ps} = 1060 \text{ m/s}$
- for the ψ wave, $V_S = 2378 \text{ m/s}$.

The source is located in the acoustic layer, at 500 m from the interface. It is a point source in space and a fifth derivative of a Gaussian of dominant frequency $f_0 = 15 \text{ Hz}$:

$$f(t) = 4.10^{10} \frac{\pi^2}{f_0^2} \left[9 \left(t - \frac{1}{f_0} \right) + 4 \frac{\pi^2}{f_0^2} \left(t - \frac{1}{f_0} \right)^3 - 4 \frac{\pi^4}{f_0^4} \left(t - \frac{1}{f_0} \right)^5 \right] e^{-\frac{\pi^2}{f_0^2} \left(t - \frac{1}{f_0} \right)^2}.$$

We compute the solution at two receivers, the first one is in the acoustic layer, at 533 m from the interface; the second one is in the poroelastic layer, at 533 m from the interface; both are located on a vertical line at 400 m from the source (see Fig. 6). We represent the y component of the displacement from $t = 0$ to $t = 1 \text{ s}$. on Fig 7. The left picture represents the solution at receiver 1 while the right picture represents the solution at receiver 2. On both pictures the blue solid curve is the analytical solution and the red dashed curve is the numerical solution.

Both pictures show a good agreement between the two solutions.

4 Conclusion

In this paper we have provided the complete solution (reflected and transmitted wave) of the propagation of wave in a stratified 2D medium composed of an acoustic and a poroelastic layer and we have validated the solution through comparison with a numerical solution. In a forthcoming paper we will use this solution as a basis to derive the solution in a three dimensional medium. We will also extend the method to the propagation of waves in heterogeneous poroelastic medium in two and three dimensions (the two-dimensional case has already been implemented in the code Gar6more 2d).

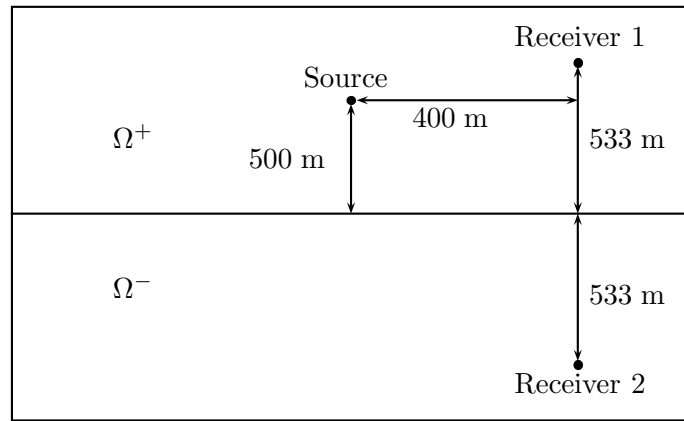
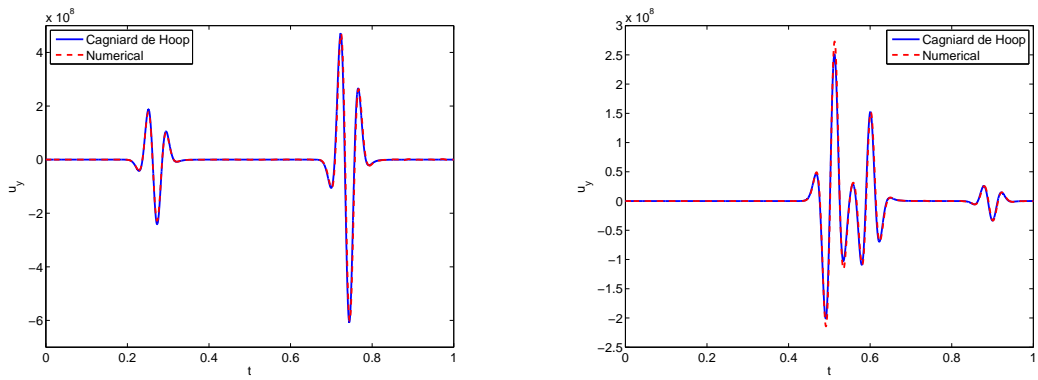


Figure 6: Configuration of the experiment

Figure 7: The y component of the displacement at receiver 1 (left picture) and 2 (right picture). The blue solid curve is the analytical solution computed by the Cagniard-de Hoop method, the red dashed curve is the numerical solution.

Acknowledgments

We thanks Christina Morency who provided us the numerical solutions we have used to validate our analytical solution.

References

- [1] M. A. Biot. Theory of propagation of elastic waves in a fluid-saturated porous solid. I. low-frequency range. *J. Acoust. Soc. Am.*, 28:168–178, 1956.
- [2] M. A. Biot. Theory of propagation of elastic waves in a fluid-saturated porous solid. II. higher frequency range. *J. Acoust. Soc. Am.*, 28:179–191, 1956.
- [3] M. A. Biot. Mechanics of deformation and acoustic propagation in porous media. *J. Appl. Phys.*, 33:1482–1498, 1962.
- [4] L. Cagniard. *Reflection and refraction of progressive seismic waves*. McGraw-Hill, 1962.
- [5] J. M. Carcione. *Wave Fields in Real Media : Wave propagation in Anisotropic, Anelastic and Porous Media*. Pergamon, 2001.
- [6] A. T. de Hoop. The surface line source problem. *Appl. Sci. Res. B*, 8:349–356, 1959.
- [7] J. Diaz. *Approches analytiques et numériques de problèmes de transmission en propagation d'ondes en régime transitoire. Application au couplage fluide-structure et aux méthodes de couches parfaitement adaptées*. PhD thesis, Université Paris 6, 2005.
- [8] J. Diaz and A. Ezziani. Gar6more 2d.
<http://www.spice-rtn.org/library/software/Garcimore2D>, 2008.
- [9] A. Ezziani. *Modélisation mathématique et numérique de la propagation d'ondes dans les milieux viscoélastiques et poroélastiques*. PhD thesis, Université Paris 9, 2005.
- [10] S. Feng and D. L. Johnson. High-frequency acoustic properties of a fluid/porous solid interface. ii. the 2d reflection green's function. *J. Acoust. Sec. Am.*, 74(3):915–924, 1983.
- [11] Q. Grimal. *Etude dans le domaine temporel de la propagation d'ondes élastiques en milieux stratifiés ; modélisation de la réponse du thorax à un impact*. PhD thesis, Université Paris12-Val de Marne, 2003. in french.
- [12] C. Morency and J. Tromp. Spectral-element simulations of wave propagation in porous media. submitted.
- [13] Y. Pao and R. Gajewski. *The generalized ray theory and transient response of layered elastic solids*, volume 13 of *Physical Acoustics*, chapter 6, pages 183–265. 1977.
- [14] J. H. M. T. van der Hadden. *Propagation of transient elastic waves in stratified anisotropic media*, volume 32 of *North Holland Series in Applied Mathematics and Mechanics*. Elsevier Science Publishers, 1987.

Contents

| | | |
|----------|---|-----------|
| 1 | The model problem | 3 |
| 1.1 | The equation of acoustics | 3 |
| 1.2 | Biot's Model | 4 |
| 1.3 | Transmission conditions | 5 |
| 1.4 | The Green problem | 6 |
| 2 | Computation of the analytical solution | 8 |
| 2.1 | Notations | 8 |
| 2.2 | Main result | 14 |
| 2.3 | Proof of the theorem | 16 |
| 3 | Comparison with a numerical solution | 22 |
| 4 | Conclusion | 22 |



Centre de recherche INRIA Bordeaux – Sud Ouest
Domaine Universitaire - 351, cours de la Libération - 33405 Talence Cedex (France)

Centre de recherche INRIA Grenoble – Rhône-Alpes : 655, avenue de l'Europe - 38334 Montbonnot Saint-Ismier

Centre de recherche INRIA Lille – Nord Europe : Parc Scientifique de la Haute Borne - 40, avenue Halley - 59650 Villeneuve d'Ascq

Centre de recherche INRIA Nancy – Grand Est : LORIA, Technopôle de Nancy-Brabois - Campus scientifique

615, rue du Jardin Botanique - BP 101 - 54602 Villers-lès-Nancy Cedex

Centre de recherche INRIA Paris – Rocquencourt : Domaine de Voluceau - Rocquencourt - BP 105 - 78153 Le Chesnay Cedex

Centre de recherche INRIA Rennes – Bretagne Atlantique : IRISA, Campus universitaire de Beaulieu - 35042 Rennes Cedex

Centre de recherche INRIA Saclay – Île-de-France : Parc Orsay Université - ZAC des Vignes : 4, rue Jacques Monod - 91893 Orsay Cedex

Centre de recherche INRIA Sophia Antipolis – Méditerranée : 2004, route des Lucioles - BP 93 - 06902 Sophia Antipolis Cedex

Éditeur

INRIA - Domaine de Voluceau - Rocquencourt, BP 105 - 78153 Le Chesnay Cedex (France)

<http://www.inria.fr>

ISSN 0249-6399